First principle study of Er, co-doped Fe and Yb of NaBiF₆; a promising materials for optoelectronic and transport properties; probed by DFT

S. Ullah[a], S. Azam[b,*], B. Gul[c], F. Subhan[d,e], S. Muhammad[a],
A. Dahshan[f,g], S. S. Ahmad[h], A. Kalsoom[i], S. Faisal[e], H. H. Hegazy[f]
[a]*Department of Physics, Hazara University, Mansehra, Pakistan*
[b]*Faculty of Engineering and Applied Sciences, Department of Physics, RIPHAH International University, Islamabad, Pakistan*
[c]*National University of Sciences and Technology (NUST), Islamabad, Pakistan*
[d]*Department of Physics, Abdul Wali Khan University, Mardan, Pakistan*
[e]*Government Post Graduate College, Swabi, Pakistan*
[f]*Department of Physics - Faculty of Science - King Khalid University, P.O. Box 9004, Abha, Saudi Arabia.*
[g]*Department of Physics, Faculty of Science, Port Said University, Port Said, Egypt.*
[h]*Department of Physics, University of Swabi, Pakistan*
[i]*Department of Physics, The Government Sadiq College Women University, Bahawalpur, Pakistan*

Despite of getting higher efficiencies from hybrid perovskite solar cells, it is necessary to investigate stable and desirable bandgap materials. We introduced new promising class of double perovskites (DPs) materials using density functional theory predictions, for solar cells applications. The results of band structure show that Er along with the co-doped Fe and Yb of NaBiF₆ with intermetallic nature. The optical properties have studied by considering interband transitions, where many levels of optical transitions is observed. We calculated optical dispersions e.g real and imaginary parts of complex dielectric function, energy loss function, reflectivity, absorption coefficient, refractive index and optical conductivity as function of photon energy from 0 to 14 eV for both spins up and down polarizations. The investigated materials contains high spin symmetry except at low energies, weakly photons reflected in IR and visible regions and absorb photons strongly in the UV region. These optical properties may be used for applications in optoelectronic devices.

1. Introduction

Light plays a vital in the progress of humanity, therefore, light emitting diodes (LED's) are involved in many applications of daily life like energy-efficient lighting by warm white-LED's (WLED's) and display backlights for tablets, televisions and smartphones. The significance of WLED's was acknowledged by awarding Noble Prize of Physics in 2014 for the discovery of efficient blue LED's which is energy saving as well as bright source of white light[1].Recently, WLED's have extensively been used in illumination systems due to their distinct characteristics. LED's based illumination systems are more environment friendly, more efficient and more durable (>100,000 hours) as compared to traditional systems[2-6]. Phosphors are the materials of keen interest for researchers as they can be potential raw materials for LEDs. Normally, yellow phosphor YAG:Ce³⁺(Y₃Al₅O₁₂:Ce³⁺) are combined with blue LED chip to produce common LED but have many limitations regardless of its easy fabrication and low cost. Therefore, color rendering index is enhanced by adding some rare-earth (RE) metal doped red phosphors like Sr₂Si₅N₈:Eu²⁺ and CaAlSiN₃:Eu²⁺[7, 8]. Recently, hexafluorosilicatephosphors doped with

---

Mn^{4+}like ASiF$_6$:Mn^{4+}(A = Ba, Zn) and B$_2$SiF$_6$:Mn^{4+} (B = Na, K, Cs)have attracted remarkable attention of the researchers.

Due to lower thermal quenching at high temperature and high efficiency at room temperature, a red-emitting KSF (K$_2$SiF$_6$:Mn^{4+})phosphor is proposed to be a potential candidate that will maximize the luminous efficiency of LED's and produce a broad gamut in the display field [9-11].Mu-Huai Fang*et. Al.*[12]used co-precipitation method in order to synthesize a new Rb$_2$SiF$_6$:Mn^{4+} phosphor. High color purity, high thermal stability and red-line emission spectrum were the key properties of this phosphor, therefore, this phosphor will be a potential candidate for enhancement of color rendering index of LED devices. Enhai Song*et. Al.*[13]presented their study on Cs$_2$SiF$_6$:Mn^{4+}phosphor while synthesizing stable narrow band red phosphor with high efficiency for its potential applications in high-power warm white LED.

In this article, we performed DFT calculations in order to calculate optoelectronic properties of Er along with the co-doped Fe and Yb of NaBiF$_6$ for prospective photovoltaic applications with the help of GGA approach by using full potential augmented plane wave (FP-LAPW) method. This study provides more information regarding physical properties of these phosphors for photovoltaic applications.

2. Computational details

Crystalline structures of Er along with the co-doped Fe and Yb of NaBiF$_6$ as shown in Fig. 1, having space group Fm-3m. These crystals have cubic symmetry with lattice parameters a=b=c=12.11Å and α=β=γ=90º. Full potential linearized augmented plane wave (FP-LAPW) method is used in order to calculate optoelectronic properties of Er along with the co-doped Fe and Yb of NaBiF$_6$ within the framework of density functional theory (DFT) [14, 15] as implemented in WEIN2K code [16, 17].DFT based computational tools are among most effective tools for calculations of ground states properties of various compounds. Exchange-correlation potential is calculated by using generalized gradient approximation (GGA) as results produced by GGA are better than local density approximation (LDA) method [18]. In this article, GGA scheme is used for the calculations of electronic and optical properties of aforesaid ternary compounds.

In FP-LAPW scheme, two regions are used to explain unit cell of the compounds under study (i) muffin-tins (atomic spheres) and (ii) interstitial region (IR). Region outside muffin-tin spheres is known as interstitial region (IR). Wave function is expanded with the help of two entirely different basis sets. Plane wave basis and radial function time's spherical harmonics (atomic-like functions) are used for the expansion of wave function in the interstitial regions (IR) and inside each muffin-tin sphere, respectively[19]. Inside the atomic sphere, maximum value of angular momentum is taken as $l_{max} = 10$ to expand wave function. Fully relativistic and semi-relativistic approachesare used to treat core and valance electrons, respectively [19]. These values of R_{MT} are selected to ensure no charge-leakage from the core and the convergence of total energy. In interstitial region, $R_{MT}.k_{max} = 7$ is taken as the cut-off value for plane wave and a k-mesh of 500 points are taken for the calculations of optoelectronic properties of aforementioned compounds.
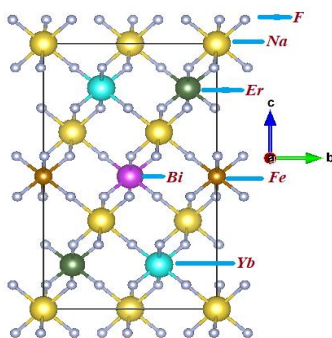

Fig. 1. Crystal structure of Er along with the co-doped Fe and Yb of NaBiF$_6$.

2.1. Density of states

To expand the spectroscopic properties several functionals were gradually applied to the nanomaterial as follows first the classical picture in the generalized gradient approximation (GGA) with the Perdew–Burke–Ernzerhof (PBE) functional was used [20].

The effect of Ce (4f) electron correlation was involved by considering on-site Coulomb (U) and exchange (J) interactions following the approach described previously [21-22]. The average value of the effective term for doped Er along with the co-doped Fe and Yb of NaBiF$_6$ was measured which was U–J = 7 eV [23-24]. Then the semi-local modified functional Becke–Johnson potential (TB-mBJ) developed by Tran and Blaha was used [25]. Spin-polarized calculations were also done using the spin orbit coupling (SOC) familiar density functional theory in order to explore the role played by the Fe-d and Er-f localized electrons [26-27].
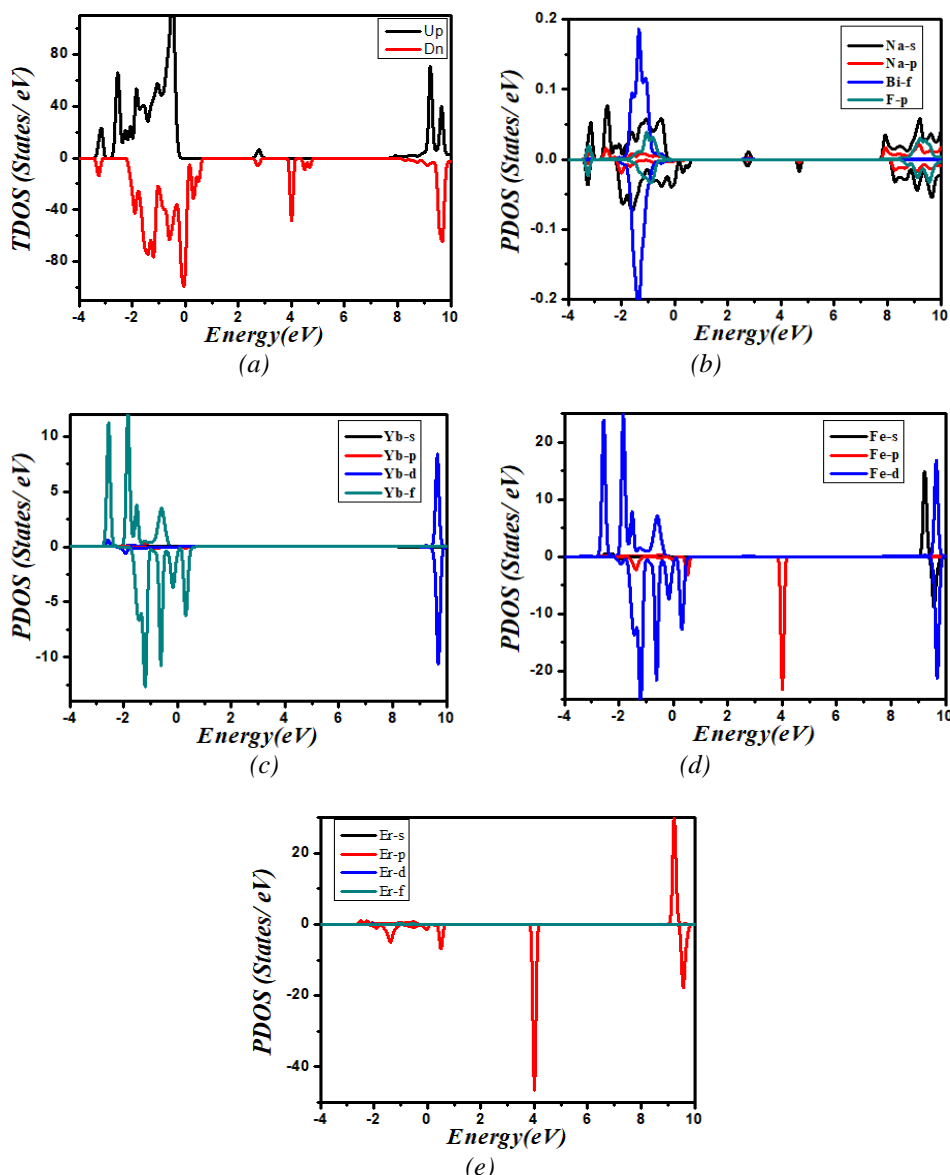

Fig.2 (a) Total density of states Er along with the co-doped Fe and Yb of NaBiF$_6$, (b-e) Partial density of states

So as to illuminate the main contribution of orbit in the band structure, the total and partial density of states (DOS) are calculated. We can acquire the pure representation for the electronic

band structure, from the computed total and partial density of states. The plots for the total and partial density of states (TDOS & PDOS) are depicted in Fig.

The total density of states (TDOS) and the partial density of states (PDOS) are attained by projection on the orbitals within the muffin tin (MT) spheres of radius R_{mt}, are shown in Fig. The Fermi level is reserved as the center of the energy. Note that results for spin-up and spin-down calculations are distinguishable. The total DOS shows the presence of relatively broad bands for the energy values between -4eV and 0eV and between 1eV and 10eV, a more complex structure with several delocalized states are above 5eV. PDOS analysis shows that optical properties is mostly related is due to strong hybridization between Yb (f) and Fe (d) states below E_F in valance band and other peaks of PDOS are from hybridization between Fe (d) and Yb (d) above E_F in conduction band. The contributions of other orbitals of Er (p) and Fe (p) are minor.

2.2. Optical properties

The light interacts with matter in many ways whose effects are of great interest for materials. The optical properties of solids give a significant means for studying localized defects, excitons, lattice vibrations, energy band structure, impurity levels, and certain magnetic excitations. When light of particular energy falls on the materials surface transition of electrons takes place between the occupied valence bands and the unoccupied conduction bands. These transition acts as source of information about the energy bands. This is the reason that energy dependent optical properties are related with band structure. To calculate the optical properties of materials there are some properties which tell us about that a compound is how much is optically active?

Optical properties such as the dielectric function, refraction index, reflectivity, refractive function and transmittance as a function of frequency have been widely studied [28-29]. Important experimental studies have confirmed some specific properties that were previously predicted by theory, such as the nature of the chemical bond in $[NaBiF_6]$: Er, Fe,Yb or electron transfer between atoms.

These properties are detailed below for $[NaBiF_6]$: Er, Fe,Yb using mBJ+U approximations in Win2K software.

2.3. Dielectric function

The major calculation for theoretical investigation of the optical properties is the dielectric function. The dielectric function of a material defines the electrical and optical properties versus frequency, wavelength, or energy. It describes the polarization (electric polarizability) and absorption properties of the material. The dielectric function $\varepsilon(\omega)$, is the combination of two parts $\varepsilon_1(\omega)$ and $\varepsilon_2(\omega)$.

$$\varepsilon(\omega) = \varepsilon_1(\omega) \pm i\varepsilon_2(\omega)$$

$\varepsilon(\omega)$ is the complex dielectric function and ω is angular frequency. Note $\varepsilon_2(\omega)$ is sometimes written as a positive quantity, or sometimes as a negative quantity so, the equation above contains $\pm$ to cover either case. The quantity $\varepsilon_1(\omega)$ represents how much a material becomes polarized when an electric field is applied?

The imaginary part of the dielectric tensor is directly related to the electronic band structure and can be computed using the one-electron orbitals and energies obtained by solving the Kohn–Sham equations. It is calculated using the following relation.

$$\varepsilon_2(\omega) = \left(\frac{4\pi^2 e^2}{m^2\omega^2}\right) \sum_{ij} \int_{BZ} <i|M|j>^2 F_i(1-F_j)\, \delta(E_F - E_i - \omega) d^3k$$

where e is the electron charge, m the free electron mass, ω is the frequency, i and j are the initial and final states respectively, M represents the dipole matrix, F_i is the Fermi distribution function for the ith state, and E_i is the energy of an electron in the ith state. The dielectric function describes a causal response, so the real and imaginary parts are linked by a Kramers–Kronig transformation.

The real part is also given as

$$\varepsilon_1(\omega) = \quad 1 + \frac{2}{\pi} \; P \int\limits_0^\infty \frac{\omega' \varepsilon_2(\omega')}{\omega'^2 - \omega^2} \, d\omega'$$

where 'P' is the principal value of the integration. When the induced dipole oscillations in a material become large it is possible for the material to start absorbing energy from the applied field. When absorption occurs the quantity $\varepsilon_2(\omega)$ becomes important. When a material is transparent $\varepsilon_2(\omega)$ is zero, but becomes nonzero when absorption begins.

It is important to consider both $\varepsilon_1(\omega)$ and $\varepsilon_2(\omega)$ together since they affect each other, meaning the shape of $\varepsilon_2(\omega)$cause corresponding changes in the shape of $\varepsilon_1(\omega)$ and vice-versa. This is known as the Kramers-Kronig relation between the real $\varepsilon_1(\omega)$ and imaginary $\varepsilon_2(\omega)$ parts of the dielectric function. In short, the dielectric function describes what an electric field such as an oscillating light wave does to material. ε_1 = volume polarization term Dipoles created. $\varepsilon2$ = volume absorption vibrational energy lost as heat in insulating materials, or electrons become free carriers in solar cells, for example. The dielectric function is related to the refractive index of a material by the equation.
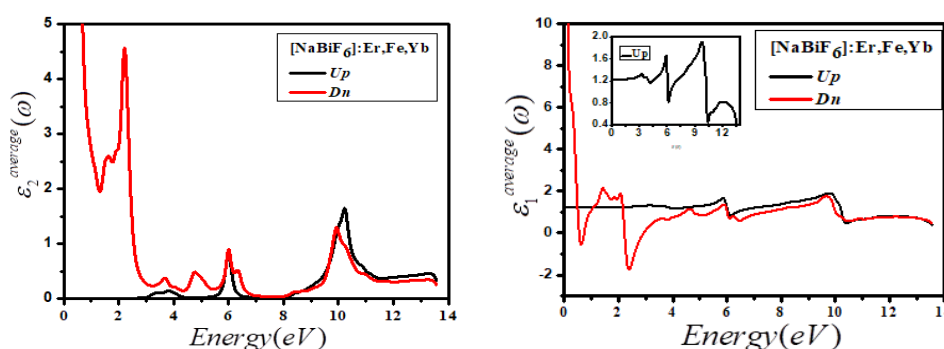
$$\varepsilon = n^2$$

Fig. 4. (a-b) Dielectric (function Real and Imaginary) using mBJ+U.

From imaginary dielectric function for up and down spin, we see that at lower value of energies 0.0eV to 3.0eV greater effect is being occur at dielectric function but after 3.0eV of energy an abrupt variation occurs in $\varepsilon_2(\omega)$. The most important point for real part is reference line adjusted at 0 values.

2.4. Absorption coefficient $I(\omega)$

Several studies have reported on absorbance and reflectance spectra of $[NaBiF_6]$: Er, Fe,Yb-based materials [30-34]. Measurement of the absorption of light is one of the most significant procedures for optical measurements in solids. In its measurements, we are focused with the light intensity I(z) after penetration of a thickness (z) of compound as compared with the incident intensity I_0, which is defined as the absorption coefficient

$$I(z) = I_0 e^{-\alpha(\omega)z}$$

The absorption spectrum I (ω) is plotted in Fig. in the energy range of 0.0 -14.0 eV, the spectrum reveals that the deep absorption occurs at high energies. It might be caused by the electronic transitions which takes place only in response to a definite energy of photon and monitor the selection rules. The absorption's first peak originates at 0.0 and 3.0 eV for down and up states and many transitions takes place after 3.0eV and goes to 11eV but after this energy absorption starts immediately higher and terminates at 14eV. This energy range is in UV region. Our calculations show that bulk $[NaBiF_6]$: Er, Fe,Yb absorbs more energy in UV region.
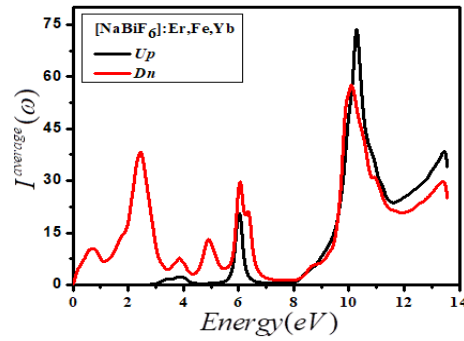
Fig. 5. Absorption spectra using GGA+U and mBJ+U.

2.5. Reflectivity R(ω)

Another important property of material is reflectivity of light by investigated compound in the 0.0eV - 14eV of energy. As calculation is carried out in the presence of magnetic field so, up and down spin behavior of material is also given in fig.
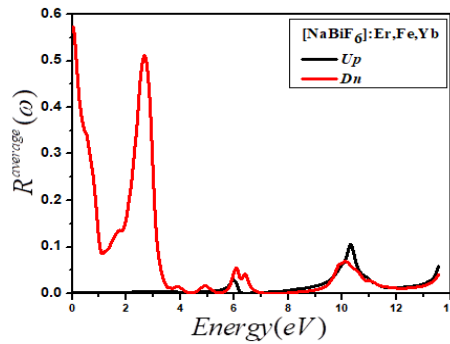

Fig. 6. Reflectivity behavior using mBJU.

The reflectivity is related to dielectric function and it is given as,

$$R= \frac{(n-1)^2 + k^2}{(n+1)^2 + k^2}$$

where n= Re$\sqrt{\varepsilon}$ and k = Im$\sqrt{\varepsilon}$, an electromagnetic wave may not penetrate into the bulk of a metal for $\omega < \omega_p$ (plasma frequency) and it reflects. The maximum reflectivity takes place where the real part of dielectric function $\varepsilon_1(\omega)$ becomes negative. In the above characteristics of reflectivity we see that in the energy range 0.0eV - 3.5eV we see the maximum reflectivity for down state. But after this energy i.e higher energy values it does not change linearly up to about 14eV. We can also see from dielectric function that at 12 eV energy real part of dielectric function become negative and reflectivity start toward maximum value.

2.6. Energy loss Function L(ω)

The excitations in the solid are also predicted by the energy losses of the electrons, when a beam of mono energetic electrons imposes on a solid [35].

The energy losses, whether created from inter-band transitions, excitons creation, Plasmon excitations or any other excitation, are material's specific. The initial electron energy has no influence on the values of the energy losses. It is the expense of energy by fast moving electron in a material. This is also related to imaginary part of dielectric function i. e.

$$L(\omega) = -\frac{1}{\varepsilon_2} = \frac{\varepsilon_2}{\varepsilon_1^2 + \varepsilon_2^2}$$

Fig. shows the behavior of energy loss as a function of frequency and energy in eV. We see that as energy increases, there is no effect on this function up to 0eV – 4.0eV for spin up, but for the spin down we can see a maximum loss at 3.0 eV. Above 6.0 eV there is no change for both spins.
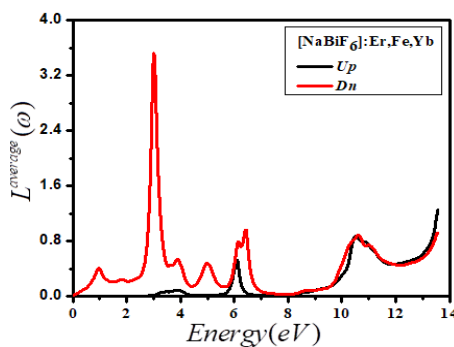

Fig. 7. Energy loss Function L(ω).

3. Conclusion

The main intention of our study is to analyze electronic and optical properties of Er along with the co-doped Fe and Yb of $NaBiF_6$ compounds using first principles calculations. The simulation code used for such calculations is Wien 2k, in which FP-LAPW method implemented. Firstly, we optimized structure of both materials by GGA-PBE as exchange correlation energy functional. The band structure calculations exhibit intermetallic nature. PDOS analysis shows that optical properties is mostly related is due to strong hybridization between Yb (f) and Fe (d) states below E_F in valance band and other peaks of PDOS are from hybridization between Fe (d) and Yb (d) above E_F in conduction band. The contributions of other orbitals of Er (p) and Fe (p) are minor. The optical dispersive constants exhibit that both materials absorb UV photons efficiently. The spectral analysis show strong absorption in the ultraviolet region. The value of reflectivity is low in IR to visible region, while strong reflectivity is observed in UV part of spectrum. So, these materials are suitable in anti –reflection coatings and photo-oxidative degradation inhibiter applications.

References

[1] A. B. Nobel Media, The 2014 Nobel Prize in Physics - Press Release, http://www.nobelprize.org/nobel_prizes/physics/laureates/2014/press.html.
[2] W. T. Chen, H. S. Sheu, R. S. Liu, J. P. Attfield, J. Am. Chem. Soc. **134**, 8022 (2012).
[3] W. B. Park, S. P. Singh, C. Yoon, K. S. Sohn, J. Mater. Chem. C **1**, 1832 (2013).
[4] H. Daicho, T. Iwasaki, K. Enomoto, Y. Sasaki, Y. Maeno, Y. Shinomiya, S. Aoyagi,

E. Nishibori, M. Sakata, H. Sawa, S. Matsuishi, H. Hosono, Nat. Commun. **3**, 1132 (2012).

[5] C. Y. Sun, X. L. Wang, X. Zhang, C. Qin, P. Li, Z. M. Su, D. X. Zhu, G. G. Shan, K. Z. Shao, H. Wu, J. Li, Nat Commun **4**, 2717 (2013).

[6] C. W. Yeh, W. T. Chen, R. S. Liu, S. F. Hu, H. S. Sheu, J. M. Chen, H. T. Hintzen, J. Am. Chem. Soc. **134**, 14108 (2012).

[7] X. Q. Piao, T. Horikawa, H. Hanzawa, K. Machida, Appl. Phys. Lett. **88**, 161908 (2006).

[8] K. Uheda, N. Hirosaki, Y. Yamamoto, A. Naito, T. Nakajima, H. Yamamoto, Electrochem. Solid-State Lett. **9**, H22 (2006).

[9] J. W. Moon, B. G. Min, J. S. Kim, M. S. Jang, K. M. Ok, K.-Y. Han, J. S. Yoo, Opt. Mater. Express **6**, 782 (2016).

[10] H. Zhu, C. C. Lin, W. Luo, S. Shu, Z. Liu, Y. Liu, J. Kong, E. Ma, Y. Cao, R.-S. Liu, Nat. Commun. 5, (2014).

[11] M. J. Lee, Y. H. Song, Y. L. Song, G. S. Han, H. S. Jung, D. H. Yoon, Mater. Lett. **141**, 27 (2015).

[12] M. H. Fang, H. D. Nguyen, C. C. Lin, R. S. Liu, Journal of Materials Chemistry C **3**(28), 7277 (2015).

[13] E. Song, Y. Zhou, X. B. Yang, Z. Liao, W. Zhao, T. Deng, Q. Zhang, Acs Photonics **4**(10), 2556 (2017).

[14] P. Hohenberg, W. Kohn, Phys. Rev. B **136**, 864 (1964).

[15] W. Kohn, L. J. Sham, Phys. Rev. **140**, A1133 (1965).

[16] P. Blaha, K. Schwarz, P. Sorantin, S. K. Trickey, Comput. Phys. Commun. **59**, 339 (1996).

[17] P. Blaha, K. Schwarz, G. H. Madsen, D. Kbasnicka, J. Luitz, 2001 ed K Schwarz FP-LAPW+lo Program for Calculating Crystal Properties,Techn. (Austria: WIEN2K)

[18] S. Azam, M. Irfan, Z. Abbas, M. Rani, T. Saleem, A. Younus, A. G. Al-Sehemi, Materials Research Express **6**(11), 116314 (2019).

[19] S. Azam, M. Irfan, Z. Abbas, S. A. Khan, I. V. Kityk, T. Kanwal, A. G. Al-Sehemi, (Se) Journal of Alloys and Compounds **790**, 666 (2019).

[20] J. P. Perdew, K. Burke, M. Ernzerhof, Phys. Rev. Lett. **77**, 3865 (1996).

[21] V. I. Anisimov, J. Zaanen, O. K. Andersen, Phys. Rev. B: Condens. Matter Mater. Phys. **44**, 943 (1991).

[22] J. Z. V. I. Anisimov, O. K. Andersen, Phys. Rev. B: Condens. Matter Mater. Phys. **44**, 943 (1991).

[23] Y. Jiang, J. B. Adams, M. van Schilfgaarde, J. Chem. Phys. **123**, 064701 (2005).

[24] C. Loschen, J. Carrasco, K. M. Neyman, F. Illas, Phys. Rev. B: Condens. Matter Mater. Phys. **75**, 035115 (2007).

[25] F. Tran, P. Blaha, Phys. Rev. Lett. **102**, 226401 (2009).

[26] F. Tran, P. Blaha, K. Schwarz, P. Novak, Phys. Rev. B: Condens. Matter Mater. Phys. **74**, 155108 (2006).

[27] F. Tran, P. Blaha, Phys. Rev. B: Condens. Matter Mater. Phys. **83**, 235118 (2011).

[28] S. Guo, H. Arwin, S. N. Jacobsen, K. Jarrendahl, U. Helmersson, J. Appl. Phys. **77**, 5369 (1995).

[29] M. Marabelli, P. Wachter, Phys. Rev. B: Condens. Matter Mater. Phys. **36**, 1238 (1987).

[30] A. H. Morshed, M. E. Moussa, S. M. Bedair, R. Leonard, S. X. Liu, N. El-Masry, Appl. Phys. Lett. **70**, 1647 (1997).

[31] F. Marabelli, P. Wachter, Phys. Rev. B **36**, 1238 (1987).

[32] T. Inoue, Y. Yamamoto, S. Koyama, S. Suzuki, Y. Ueda, Appl. Phys. Lett. **56**, 1332 (1990).

[33] S. Guo, H. Arwin, S. N. Jacobsen, K. Jarrendahl, U. Helmersson, J. Appl. Phys. **77**, 5369 (1995).

[34] S. Y. Zheng, A. M. Andersoon-Faldt, B. Stjerna, C. G. Granqvist, Appl. Opt. **32**, 6303 (1993).

[35] L. Marton, L. B. Leder, H. Mendlowitz, Advances in Electronics and Electron Physics, **7**, Academic Press, New York, 1955.